ACS Medicinal Chemistry Letters

LETTER

pubs.acs.org/acsmedchemlett

# Highly Selective and Potent Thiophenes as PI3K Inhibitors with Oral Antitumor Activity

Kevin K.-C. Liu,* JinJiang Zhu, Graham L. Smith, Min-Jean Yin, Simon Bailey, Jeffrey H. Chen, Qiyue Hu, Qinhua Huang, Chunze Li, Qing J. Li, Matthew A. Marx, Genevieve Paderes, Paul F. Richardson, Neal W. Sach, Marlena Walls, Peter A. Wells, and Aihua Zou

Chemistry Department, Oncology, Pfizer Global Research and Development, 10770 Science Center Drive, La Jolla, California 92120, United States

Supporting Information

**ABSTRACT:** Highly selective PI3K inhibitors with subnanomolar PI3K$\alpha$ potency and greater than 7000-fold selectivity against mTOR kinase were discovered through structure-based drug design (SBDD). These tetra-substituted thiophenes were also demonstrated to have good in vitro cellular potency and good in vivo oral antitumor activity in a mouse PI3K driven NCI-H1975 xenograft tumor model. Compounds with the desired human PK predictions and good in vitro ADMET properties were also identified. In this communication, we describe the rationale behind the installation of a critical triazole moiety to maintain the intricate H-bonding network within the PI3K receptor leading to both better potency and selectivity. Furthermore, optimization of the C-4 phenyl group was exploited to maximize the compounds mTOR selectivity.

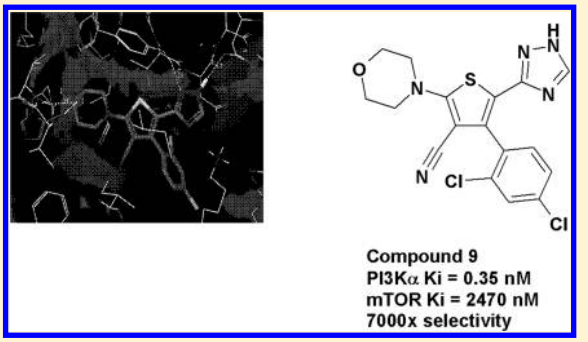


**KEYWORDS:** Kinase inhibitor, PI3K, mTOR, thiophene, triazole, antitumor activity

Phosphatidylinositol-3-kinases (PI3Ks) are lipid kinases, which phosphorylate PIP2 (phosphatidylinositol diphosphate) to PIP3 (phosphatidylinositol triphosphate), which recruits PDK and AKT to the cell membrane. AKT is activated through phosphorylation of the membrane-bound PDK leading to a myriad of downstream processes, including modulation of proteins such as mTOR (mammalian target of rapamycin), GSK3, forkhead, NF-$\kappa$B transcription factors, and eNOS. In this manner, the PI3K/AKT pathway regulates numerous processes such as metabolism, cell proliferation, growth, survival, angiogenesis, and apoptosis.[1] Aberrant activation of PI3K has been linked to both tumor initiation and maintenance. During tumorigenesis, activation of the PI3K/AKT/mTOR pathway can occur through various mechanisms, including loss of PTEN (the phosphatase that regulates PI3K signaling), overexpression or activation of certain receptor tyrosine kinases (e.g., EGFR, HER-2), interaction with activated Ras, overexpression of the PI3K-$\alpha$ gene (*PIKC3A*), or mutations in *PIKC3A* that cause elevated PI3K kinase activity.[2,3] Deregulated PI3K/AKT/mTOR pathway signaling has been implicated in poor prognosis and low survival rates in numerous forms of cancers including lymphatic tumors, glioblastomas, melanomas, breast, prostate, lung, colon, and ovarian cancers.[4] Many preclinical and clinical studies now strongly indicate that PI3K plays a key role in the biology of human cancers.[2,3] However, most of the inhibitors in this signaling pathway have inhibitory activity against both PI3K and mTOR kinases. It is known that the mTOR complexes 1 and 2 both regulate cell proliferation, apoptosis, angiogenesis, and metabolism through both AKT-dependent and AKT-independent mechanisms.[5] Agents targeting PI3Ks with additional mTOR kinase inhibitory activity may carry extra toxicity through disruption of mTOR function in normal cells. To find an inhibitor to inhibit this critical signaling pathway with a better therapeutic index, we endeavored to develop a drug selectively targeting PI3Ks.

Several chemotypes were identified with decent PI3K binding potency in our HTS assay. To derisk idiosyncratic toxicity associated with our previous PI3K/mTOR dual inhibitors,[6−8] we preferred a novel series with an available relevant cocrystal showing protein−ligand binding. This structural information would allow us to design compounds through SBDD to accelerate the lead optimization process. Compound **1**, a tetra-substituted thiophene with moderate PI3K$\alpha$ $K_i$, 230 nM (Scheme 1), was therefore picked for further investigation from other HTS hits because of its novel structure and available PI3K$\gamma$−compound **1** cocrystal structure (Figure 1). Unlike regular thiophenes that are prone to oxidative and reactive metabolites, this tetra-substituted lead compound blocks all potential oxidative sites on the thiophene core, a fact that was subsequently confirmed by our drug metabolism studies. For compounds to get good cellular potency, permeability, and absorption, our initial priority was to replace the free carboxylic acid

**Received:** June 13, 2011
**Accepted:** September 19, 2011
**Published:** September 19, 2011

**Scheme 1. Progression from Initial Thiophene HTS Hit 1 to Lead 4**[a]

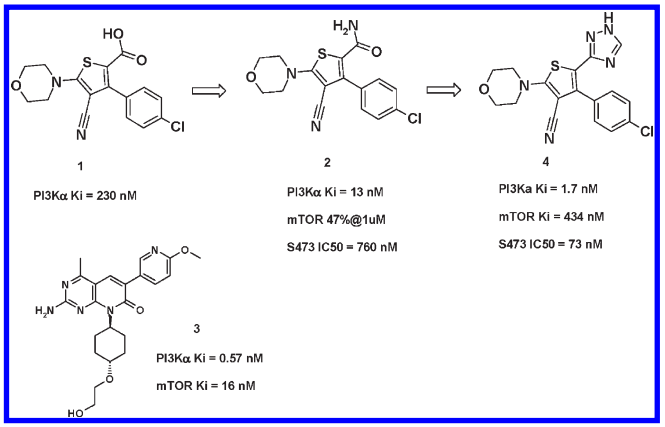


[a] Compound **3** is a dual PI3K/mTOR inhibitor (ref 6).

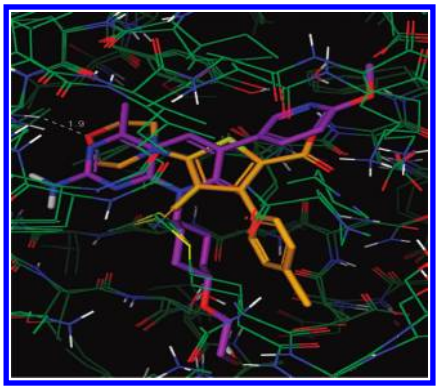

**Figure 1.** Cocrystal structures of compounds **1** (brown color) and **3** (purple color; PDB code: 3ML9) in PI3K$\gamma$. The nitrogen of the morpholine ring of compound **1** represents the kinase hinge binder.

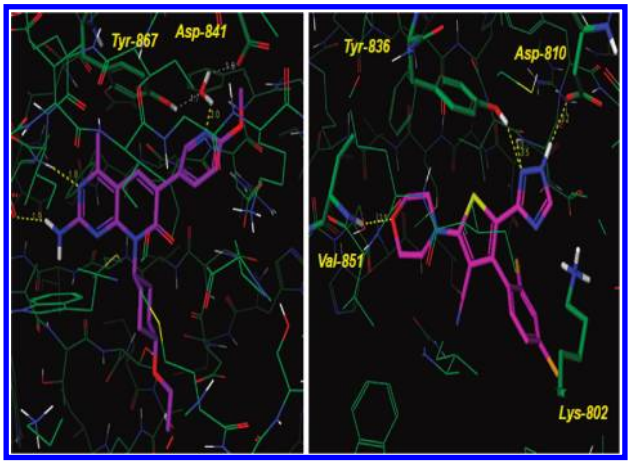


**Figure 2.** Left: compound **3** in PI3K$\gamma$ (PDB code: 3ML9). There is a water between Asp 841 and Tyr 867 to maintain a H-bonding network, and the nitrogen on the pyridine ring is making contact with this water molecule. Right: Proposed binding model for compound **4** in PI3K$\alpha$ (see the text for details).

moiety, which is known in general to be associated with both poor permeability and absorption.[9]

**Scheme 2. Proposed Binding Tautomer of Triazole, T2, Is Also the Calculated Global Minimum Energy (The Exception Being the OPLS2005 Calculation)**

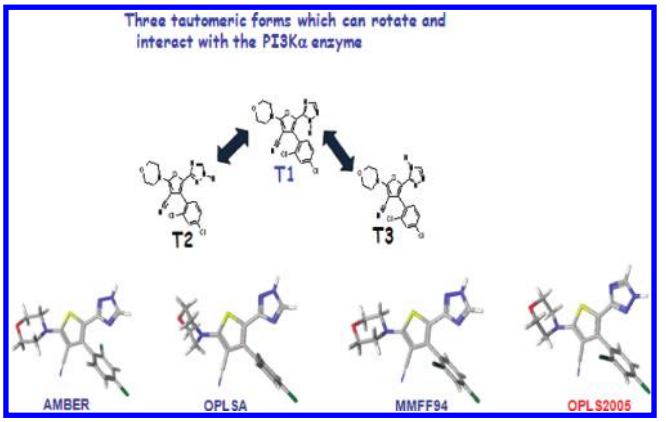


The corresponding carboxylic amide **2** was thus made, and the compound displayed a greater than 10-fold improvement on the PI3K$\alpha$ binding and less than 1 uM cellular potency in our cellular S473 AKT phosphorylation assay. In addition, compound **2** also provided good selectivity over mTOR kinase (Scheme 1). Encouraged by this result, we carefully evaluated the cocrystal structures of both compound **1** and our previously reported potent PI3K/mTOR dual inhibitors from the 4-methyl pyridopyrimidinone series.[6−8] We wanted to exploit structure−activity relationship (SAR) learnings from our dual inhibitor series and apply these to improve both potency and selectivity for our novel thiophene series. The carboxylic acid moiety of compound **1** corresponds to the methoxy pyrimidine moiety in the 4-methyl pyridopyrimidinone series as shown in the overlapped cocrystal structures in Figure 1. For clarity, compound **1** is colored in brown, and compound **3** is colored in purple. Of particular note, there is a water molecule serving as a bridge between the pyridyl nitrogen of compound **3** and the PI3K$\gamma$ enzyme. In the cocrystal structure of compound **3** shown in Figure 2 (structure on the left), there is a water molecule that sits in between the conserved Asp841 and Tyr867 residues of PI3K$\gamma$, which correspond to the Asp810 and Tyr836 residues of PI3K$\alpha$, respectively. This water molecule is making H-bonds with both the pyridyl nitrogen of compound **3** as previously mentioned and the Asp and Tyr residues in the PI3Ks, thus forming a H-bond network (Figure 2, left). To keep this intact within PI3K enzymes, a potent inhibitor needs to be designed not to disrupt this intricate H-bond network, or the inhibitor will end up losing potency because of the energy penalty paid. This observation had important ramifications on our compound designs. With this observation in mind, different amide bioisosteres were modeled and synthesized to test our hypothesis. Among these analogues, compound **4** with a 1,2,4-triazole group stands out, as this has excellent PI3K$\alpha$ $K_i$ (1.7 nM), good cellular potency (S473 $IC_{50}$ = 73 nM, Scheme 1), and good selectivity against mTOR (mTOR $K_i$ = 434 nM; 255× selectivity).

It is unfortunate that we could not obtain further cocrystal structures in this thiophene series to prove our model. However, we believe the excellent PI3K$\alpha$ potency of compound **4** is due to the 1,2,4-triazole group replacing the water molecule in the ATP-binding site, while the N1 nitrogen in the triazole functions as a H-bond acceptor to interact with Tyr836, and the N2 nitrogen

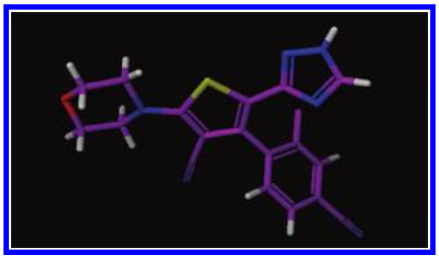

**Figure 3.** X-ray structure of compound **4**, which is consistent with both our hypothesis and computational calculations.

**Scheme 3. Amide Bioisosteric Analogues 4−8**

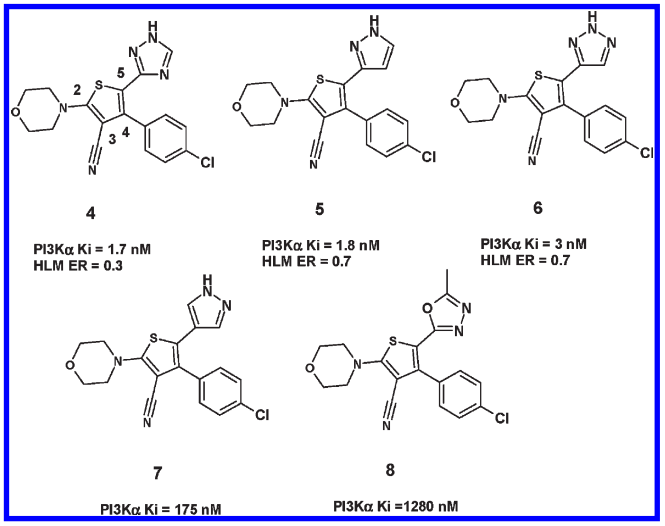


acts as a H-bond donor interacting with Asp810, thus maintaining and stabilizing the crucial PI3K$\alpha$ protein structure (Figure 2, structure on the right). The 1,2,4-triazole can exist in three different tautomeric forms as indicated in Scheme 2. Different computational calculation tools were employed to predict the preferred global minimum energy species. Three out of four calculations utilized predict **T2** as the preferred tautomeric form, which is consistent with our binding hypothesis for compound **4**. Further supporting evidence is provided by a single crystal X-ray structure of compound **4**, which also exists as the predicted **T2** tautomer (Figure 3).

The potencies of other amide bioisosteres are shown in Scheme 3. Compounds **4**−**6** display excellent potencies, whereas compounds **7** and **8** do not, which is again consistent with our H-bond donor/acceptor binding model. Compounds **4**−**6** are capable of making the H-bond acceptor/donor interactions with the aforementioned Tyr and Asp enzyme residues, respectively, but compounds **7** and **8** are not. Compound **4** further differentiates itself from compounds **5** and **6** due to its increased metabolic stability with a lower extraction ratio[10] of 0.3 vs 0.7 for compounds **5** and **6** (Scheme 3).

With these potent and stable inhibitors in hand, we then further focused to improve compound selectivity against mTOR. Both PI3K$\alpha$ and mTOR occupancy maps were generated, and these mappings suggest that the C-4 phenyl moiety partially contributes to mTOR selectivity for this series of compounds. Therefore, a library with a diverse set of aryl and heteroaryl groups on

**Table 1. Examples of Compounds from C-4 Phenyl Library: Compounds 9 and 10 with Biological and in Vitro ADME Data**

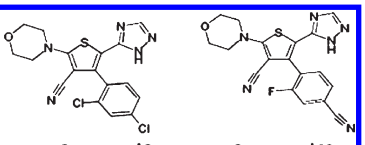

| | | Compound 9 | Compound 10 |
|---|---|---|---|
| Biochem | PI3Ka Ki (nM) | 0.35 | 0.6 |
| | mTOR Ki (nM) | 2470 | 1440 |
| cell assay | pAKT-S473 IC50 (nM) | 35 | 79 |
| | HLM ER | 0.3 | 0.35 |
| | RLM ER | 0.89 | 0.529 |
| | MLM ER | 0.88 | 0.639 |
| | RRCK | 15.8 | 16.4 |
| | MDR:BA/AB ratio | 2.56 | 2.6 |
| | cLogD | 2.81 | 1.08 |

the C-4 position was designed and synthesized after careful filtration of a series of virtual compounds to optimize a series of calculated physicochemical properties, such as clogP, molecular weight, and polar surface area.

Indeed, this C-4 aryl library generated a number of very potent compounds with excellent selectivity, that is, compounds **9** and **10** (Table 1). These two extremely potent compounds have PI3K$\alpha$ $K_i$ less than 1 nM and mTOR $K_i$ more than 1 $\mu$M. It is worth noting that compound **9** has more than 7000-fold selectivity over mTOR kinase. In addition, these two compounds also have excellent selectivity over 40 other kinases, and no major CYP inhibitions were observed. Less than 30% inhibition was observed in 1A2, 2C9, 2D6, and 3A4 CYP enzymes at 3 $\mu$M. According to the occupancy maps of PI3K$\alpha$ and mTOR shown in Figure 4, the out-of-plane 2,4-disubstituted C-4 phenyl group bumps against a region of the mTOR protein that is defined by the Ile-78, Leu-26, Lys-28, and Pro-10 residues. However, there are no such unfavorable steric interactions in the corresponding region in PI3K enzymes (Figure 4, smaller structure shown on the right). For different PI3K isoforms, these compounds have about equal potency against PI3K$\delta$ and about 10−40× less potent against PI3K$\gamma$.

The general synthesis of thiophenes and in particular compound **4** is outlined in Scheme 4 below. The synthesis started with the known compound **A**, which was prepared according to a patent procedure.[11] The thio-methyl ether **A** was subjected to *m*-CPBA oxidation to give a mixture of the sulfone and sulfoxide **B**, which was subsequently treated with morpholine to give compound **C** in 77% yield. Compound **C** was coupled with 4-chlorophenylboronic acid under optimized Suzuki conditions to give compound **D**, which was hydrolyzed under basic conditions to yield free carboxylic acid **E** in high yield. Compound **E** was then converted to the amide **2** via the acid chloride under standard conditions. Finally, compound **2** was treated with DMF and DMA at elevated temperature to give the amide ylide intermediate, which was reacted directly with hydrazine to the desired triazole **4** in 70% yield over the final two steps.[12]

From this series, compound **9** was selected for further studies due to the favorable balance of it is potency, selectivity, and physicochemical properties. Drug metabolic studies suggested that this compound would not have any issues with conjugated or

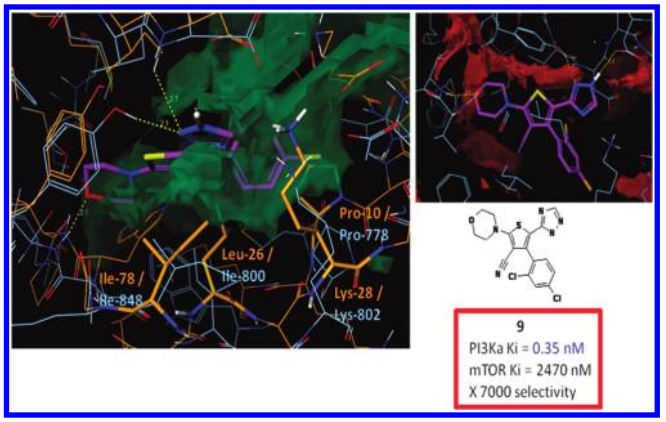


**Figure 4.** Left: mTOR protein labeled in orange and PI3K$\alpha$ labeled in light blue with surface area shown. Out-of-plane 2,4-dichlorophenyl of compound **9** impinges onto the mTOR occupancy map region defined by Ile-78, Leu-26, Lys-28, and Pro-10. Right: compound **9** shown sitting inside the PI3K$\alpha$ occupancy map.

**Scheme 4. Synthesis of Compound 4**

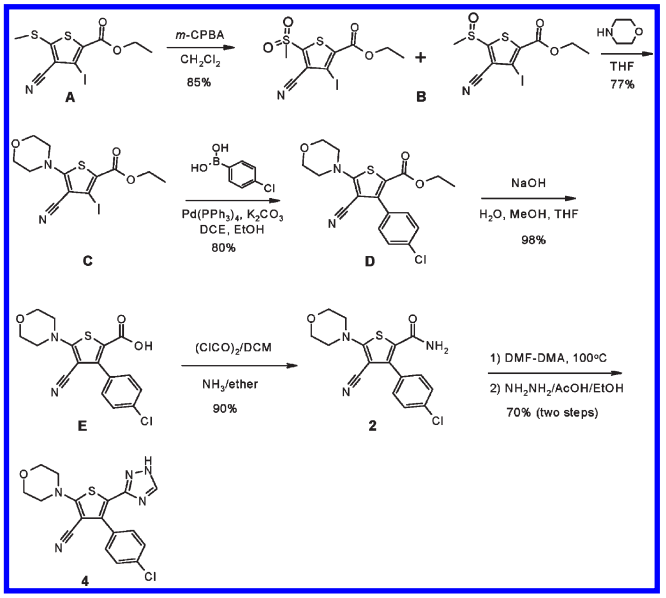


**Table 2. Human PK Predictions of Compound 9 Based on HLM**

| compd **9** | | in vitro HLM and Vdss from rats (SSS) |
|---|---|---|
| CLp | mL/min/kg | 0.52 |
| Vdss | L/kg | 1.65 |
| $t_{1/2}$ effective | h | 37 |
| *F* | % | 97 |

active metabolites. In rats with bile duct cannulation, less than 1% parent drug was excreted unchanged into urine and bile. From this data, we decided to use HLM for human PK predictions as the major metabolic pathways are clearly through oxidative transformations. Compound **9** has favorable human PK predictions with low clearance, long half-lives, and excellent bioavailability (Table 2).

**Table 3. Selective PI3K Inhibitor, Compound 9, Is More Active in NSCLCs Harboring the *PI3KCA* Mutation than Other Cancer Cell Lines**

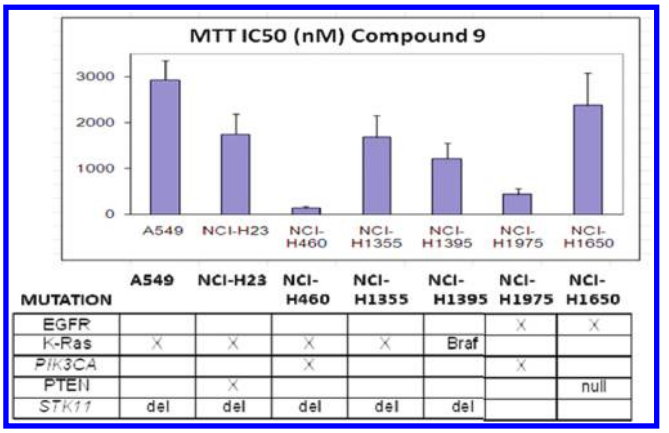


| MUTATION | A549 | NCI-H23 | NCI-H460 | NCI-H1355 | NCI-H1395 | NCI-H1975 | NCI-H1650 |
|---|---|---|---|---|---|---|---|
| EGFR | | | | | | X | X |
| K-Ras | X | X | X | X | Braf | | |
| *PIK3CA* | | | X | | | X | |
| PTEN | | X | | | | | null |
| *STK11* | del | del | del | del | del | | |

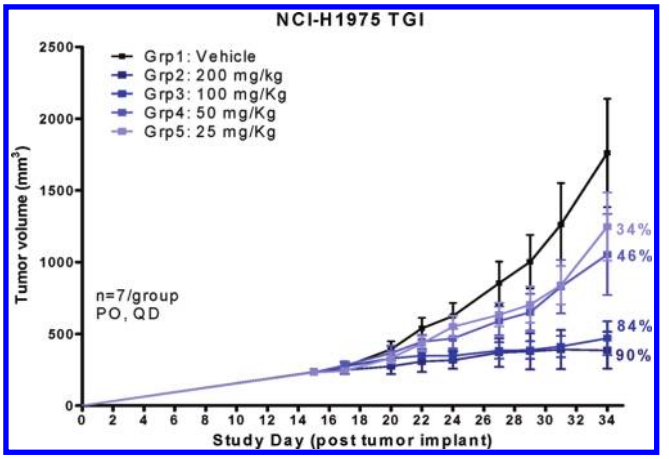


**Figure 5.** Dose−response curve of compound **10** in H1975 TGI studies.

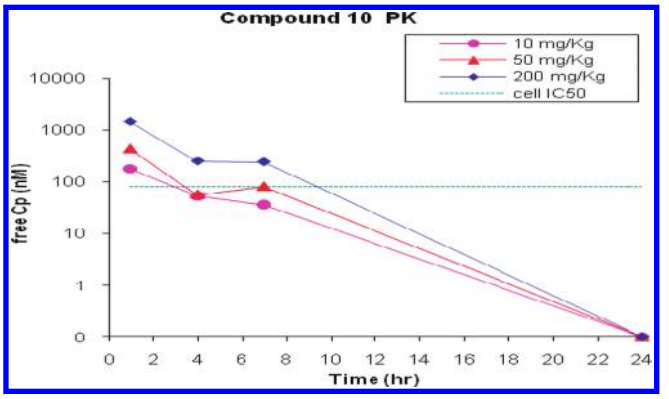


**Figure 6.** Free concentrations of compound **10** in H1975 TGI studies.

Compound **9** was tested in different cell lines for its sensitivity in the MTT cell viability assay. Interestingly, this selective PI3K inhibitor is more sensitive with the NSCLC (nonsmall cell lung cancer) cell lines that harbor *PI3KCA* mutations than cell lines with the PTEN deletion as shown in Table 3.

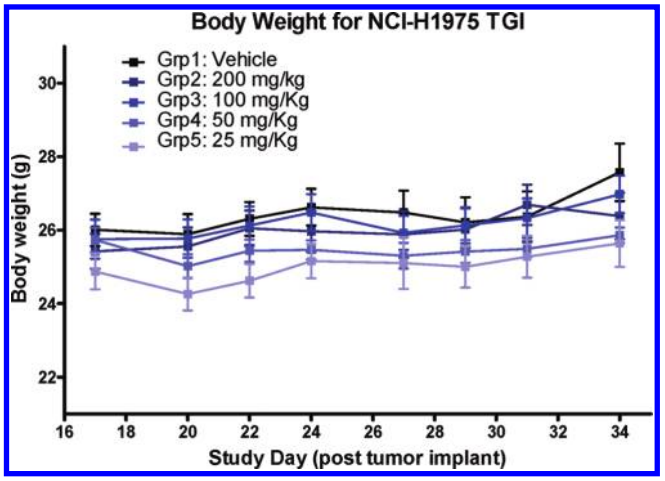


**Figure 7.** Body weight change of compound **10** in H1975 TGI studies.

Because of a better rodent PK, compound **10** was dosed orally in our in vivo antitumor model, PI3K driven NCI-H1975 xenograft tumors.[13] As shown in Figure 5, the compound demonstrated dose responsive tumor growth inhibitory activity from 25 to 200 mg/kg in QD oral dosing. In Figure 6, free concentrations of compound **10** at 50 and 200 mg have good exposures to cover the compound cell $IC_{50}$ (80 nM). There was no body weight reduction in these in vivo studies as shown in Figure 7.

In summary, structure-guided lead optimization was applied to a HTS hit to allow us to quickly discover extremely potent and selective PI3K inhibitors with novel thiophene structures. Orally active compounds with favorable human PK predictions were also identified in this series. More details regarding the optimization and development of these compounds will be disclosed in due course.

## ■ ASSOCIATED CONTENT

**Supporting Information.** Representative synthetic schemes and procedures and NMR and MS data on new compounds. This material is available free of charge via the Internet at http://pubs.acs.org.

## ■ AUTHOR INFORMATION

**Corresponding Author**
*E-mail: kevin.k.liu@pfizer.com.

## ■ ACKNOWLEDGMENT

We thank Dr. Deepak Dalvie for generating the metabolite data and Dr. Ted O. Johnson for useful discussions.

## ■ REFERENCES

(1) Engelman, J. A.; Luo, J.; Cantley, L. C. The evolution of phosphatidylinositol 3-kinases as regulators of growth and metabolism. *Nat. Rev. Genet.* **2006**, *7*, 606–619.

(2) Engelman, J. A. Targeting PI3K signalling in cancer: Opportunities, challenges and limitations. *Nat. Rev. Genet.* **2009**, *9*, 550–62.

(3) Nuss, J. M; Tsuhako, A. L; Anand, N. K. Emerging Therapies based on inhibitors of phosphatidyl-inositol-3-kinases. *Annu. Rep. Med. Chem.* **2009**, *44*, 339–356.

(4) Samuels, Y.; Wang, Z.; Bardelli, A.; Silliman, N.; Ptak, J.; Szabo, S.; Yan, H.; Gasdar, A.; Powell, S. M.; Riggins, G. J.; Willson, J. K.; Markowitz, S.; Kinzler, K. W.; Vogelstein, B.; Velculescu, V. E. High frequency of mutations of the PIK3CA gene in human cancers. *Science* **2004**, *304*, 554.

(5) Sarbassov, D. D.; Ali, S. M.; Sabatini, D. M. Growing roles for the mTOR pathway. *Curr. Opin. Cell Biol.* **2005**, *17*, 596.

(6) Cheng, H.; Bagrodia, S.; Bailey, S.; Edwards, M.; Hoffman, J.; Hu, Q.; Kania, R.; Knighton, D. R.; Marx, M. A.; Ninkovic, S.; Sun, S.; Zhang, E. *Med. Chem. Comm.* **2010**, *1* (2), 139.

(7) Liu, K. K.-C.; Huang, X.; Bagrodia, S.; Chen, J. H.; Greasley, S.; Cheng, H.; Sun, S.; Knighton, D.; Rodgers, C.; Rafidi, K.; Zou, A.; Xiao, J.; Yan, S. Quinazolines with intra-molecular hydrogen bonding scaffold (iMHBS) as PI3K/mTOR dual inhibitors. *Bioorg. Med. Chem. Lett.* **2011**, *21* (4), 1270–1274.

(8) Liu, K. K.-C.; Bagrodia, S.; Bailey, S.; Cheng, H.; Chen, H.; Gao, L.; Greasley, S.; Hoffman, J. E.; Hu, Q.; Johnson, T. O.; Knighton, D.; Liu, Z.; Marx, M. A.; Nambu, M. D.; Ninkovic, S.; Pascual, B.; Rafidi, K.; Rodgers, C. M.-L.; Smith, G. L.; Sun, S.; Wang, H.; Yang, A.; Yuan, J.; Zou, A. 4-Methylpteridinones as orally active and selective PI3K/mTOR dual inhibitors. *Bioorg. Med. Chem. Lett.* **2010**, *20* (20), 6096–6099.

(9) Kalgutkar, A. S.; Daniels, J. S. 1(Metabolism, Pharmacokinetics and Toxicity of Functional Groups), Carboxylic acids and their bioisosteres. *RSC Drug Discovery Ser.* **2010**, 99–167.

(10) $\mu$L/min/mg protein is the unit for $CL_{int}$, which can be directly obtained from the in vitro HLM experiments. We have scaled up the HLM $CL_{int}$ with known liver physiology parameters, such as mg HLM/g liver and g liver/kg body weight. Predicted hepatic clearance (CLH, mL/min/kg) was calculated with the scaled up $CL_{int}$ (mL/min/kg) using the well-stirred model. ER is the ratio of predicted CLH and hepatic blood flow (QH). As a result, the predicted ER is a parameter that directly reflects the HLM stability ($CL_{int}$ in HLM).

(11) Castano-Mansanet, A. M.; Dominguez-Manzanares, E.; Escribano, A. M.; Fernandez, M. C.; Hornback, W. J; Jimenez-Aguado, A. M.; Tromiczak, E. G.; Wu, Z.; Zarrinmayeh, H.; Zimmerman, D. M. Preparation of thiophene and furan compounds for potentiating glutamate receptor function. WO2005070916, 2005.

(12) For a detailed discussion of the synthetic chemistry, see Huang, Q; Richardson, P. F.; Sach, N. W.; Zhu, J; Liu, K. K.-C.; Smith, G. L.; Bowles, D. M. Development of Scalable Syntheses of Selective PI3K inhibitors. *Org. Process Res. Dev.* **2011**, *15* (3), 556–564.

(13) For animal studies, 6−8 week old nu/nu athymic female mice were obtained from Jackson Laboratories; the mice were maintained in pressurized ventilated caging at the Pfizer La Jolla animal facility. All studies were done in compliance with Institutional Animal Care and Use Committee guidelines. Tumors were established by injecting $2 \times 10^6$ cells suspended 1:1 (v/v) with reconstituted basement membrane (Matrigel, BD Biosciences). For tumor growth inhibition studies, mice with established tumors of ~150 $mm^3$ were randomized and orally treated with vehicle or PI3K inhibitor daily. Tumor dimensions were measured with vernier calipers, and tumor volumes were calculated using the formula: $\pi/6$(larger diameter) × (smaller diameter)$^2$. Tumor growth inhibition percentage (TGI%) was calculated as $100(1 - \Delta T/\Delta C)$.